Scripta Materialia 153 (2018) 99–103

Contents lists available at ScienceDirect

Scripta Materialia

journal homepage: www.elsevier.com/locate/scriptamat

Regular article

Early plastic deformation behaviour and energy absorption in porous β-type biomedical titanium produced by selective laser melting

Y.J. Liu [a], S.J. Li [c], L.C. Zhang [b,*], Y.L. Hao [c], T.B. Sercombe [a,*]

[a] School of Mechanical and Chemical Engineering, The University of Western Australia, 35 Stirling Highway, Perth, WA 6009, Australia
[b] School of Engineering, Edith Cowan University, 270 Joondalup Drive, Joondalup, Perth, WA 6027, Australia
[c] Shenyang National Laboratory for Materials Science, Institute of Metal Research, Chinese Academy of Sciences, 72 Wenhua Road, Shenyang 110016, China

ARTICLE INFO

Article history:
Received 21 April 2018
Received in revised form 2 May 2018
Accepted 6 May 2018
Available online xxxx

Keywords:
Selective laser melting
β titanium
Porous structures
Energy absorption
Local stress concentrations

ABSTRACT

Energy absorption is a critical consideration in the design of porous structures design. This work studied the energy absorption mechanism of three porous structures (i.e. cubic, topology optimised and rhombic dodecahedron) at the early stage of deformation. Stress distribution results, obtained by finite element modelling, coupled with the investigation of the slip bands generated have been used to reveal the plasticity mechanism and local stress concentrations for each structure. The topology optimised structure exhibits the best balance of bending and buckling stress with a high elastic energy absorption, a low Young's modulus (~2.3 GPa) and a high compressive strength (~58 MPa).

In addition to their attractive properties such as light weight and high strength, titanium alloys have been widely used as biomaterials due to their relatively low Young's Modulus, good biocompatibility and corrosion resistance [1–3].

Modern additive manufacturing (AM) technologies, such as selective laser melting (SLM) and electron beam melting (EBM), are able to produce the titanium porous implant with properties that mimic those of bone [4–7]. In recent years AM-produced titanium porous parts have attracted considerable research attention [8–18]. For example, Cheng et al. [16] investigated the open cellular structures and reticulated meshes of Ti–6Al–4 V alloy made by EBM and found that the reticulated meshes had a higher specific strength (~113 MPa with the porosity of 62%). Wang et al. [17] concluded that the AM-produced titanium porous structures would play a significant part in future human implants.

Driven by their ultra-low Young's Modulus and high strength, AM-produced β-type titanium alloys containing non-toxic elements have been emerging as the next generation candidate biomaterials [19,20]. Liu et al. [21] found that the SLM-produced β-type Ti-24Nb-4Zr-8Sn (Ti2448) porous specimens with topology optimised structures have good ductility (~14%), high strength (~51 MPa) and a low density (<1 g/cm^3). Furthermore, Ti2448 porous structures exhibit superelasticity, which is known to reduce the fatigue crack growth rate via increasing the size of plastic zone at crack tip [22]. But the shape of porous structure strongly affects the fatigue properties of porous parts. Yavari et al. [23] found that the truncated cuboctahedron structure has a higher fatigue life than the diamond structure at the same normalized applied stress. Zhao et al. [24] concluded that the strut buckling contribution and cyclic ratcheting rate are determined by the cell shape of porous structures, thereby affecting their fatigue properties. Furthermore, Bobbert et al. [25] found that the fatigue limit of porous structures can be improved to 60% of their yield stress by adjusting the unit cell design. A good porous structure can reduce stress concentrations and improve mechanical properties by adjusting bending and buckling deformation and optimizing plastic and elastic energy absorption [26,27].

Although theoretical frameworks have been established for the elastic and plastic deformation of bulk parts, no such a framework currently exists for porous structures based on the analysis of elastic and plastic energy absorption for different unit cell shapes. As such, this work concentrates on super-elasticity, early plasticity and energy absorption in different Ti2448 porous structures made by SLM. The stress distribution and local stress concentration combined with the slip band generation have also been studied.

Magics software (Materialize, Belgium) was used to produce three different 3 × 3 × 3 unit cell structures (cubic, topology optimised [4] and rhombic dodecahedron) using 3.33 × 3.33 × 3.33 mm^3 unit cells (i.e. overall size was 10 × 10 × 10 mm^3) (Fig. 1). Each structure had a nominal porosity of 80% and an as-built porosity of 75%. These porous specimens were then manufactured using SLM in a Realizer SLM100 system, with a layer thickness of 50 μm, an input energy of 200 W and

* Corresponding author.
E-mail addresses: l.zhang@ecu.edu.au, lczhangimr@gmail.com, (L.C. Zhang), tim.sercombe@uwa.edu.au (T.B. Sercombe).

https://doi.org/10.1016/j.scriptamat.2018.05.010
1359-6462/

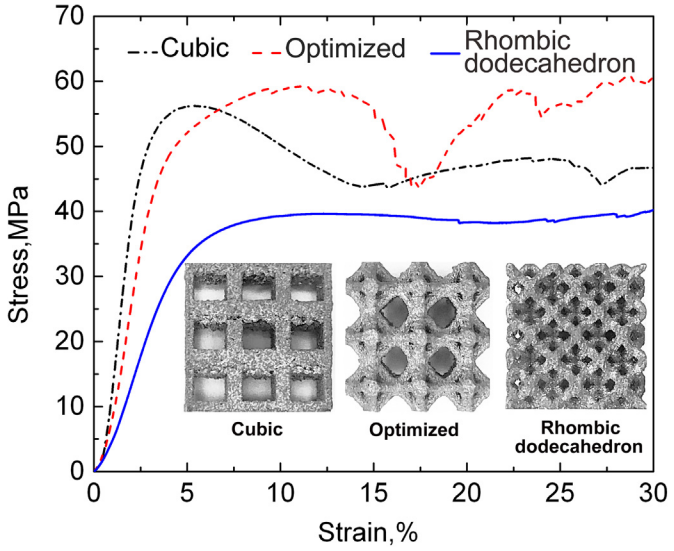

Fig. 1. The typical compressive stress-strain curves for three structures. The insets show SLM-produced samples.

a laser scan speed of 750 mm/s. The powder used was spherical Ti2448 with particle sizes of 45–106 μm, produced using electrode induction melting gas atomization (EIGA). All the samples in this work were processed in a single build. For the microstructural characterization, a specimen of each porous structure was cold mounted in using Struers' Epofix resin. The mounted specimens were ground and polished using standard metallographic procedures and finished with 0.04μm colloidal silica containing 30% hydrogen peroxide. Microstructural features were investigated by scanning electron microscopy (SEM) on a FEI Verios XHR 460 in back-scatted electron (BSE) mode. Compressive tests were performed on three samples for each group using an Instron 5982 machine at a strain rate of 0.1 mm/min. Young's Moduli (E) were measured using the unloading curves. Multiple loading tests from 1% to 6% strain were conducted at the same strain rate. During each test, the specimen was first loaded up to a 1% strain level, completely unloaded and then loaded again to 2% strain. This was continued at 1% step up to 6% strain (i.e. 6-cyclic loading-unloading tests on each sample). Finite element modelling (FEM) was carried out using Comsol 4.2a software. Three different $3 \times 3 \times 3$ unit cell models were used to study the stress distribution. The compressive load was loaded on the top surface of sample paralleled to Z axis (i.e. the build direction). The bottom boundary was fixed in the Z direction to simulate the effect of loading conditions and the rest of the boundaries were set as free, which was similar to the conditions in uniaxial compressive testing.

The typical compressive stress-strain curves for three different structures are shown in Fig. 1. Previous studies showed that similar SLM-produced Ti2448 porous structures consisted of a single β phase [19]. Therefore, it is expected that all three structures should also comprise of a single β phase. Nevertheless, these three structures exhibit different levels of ductility. The topology optimised and cubic structures have a similar first maximum compressive strength (~58 MPa and ~56 MPa, respectively). However, they undergo a very different deformation strain before the first layer-wise failure occurs, with a value of ~15% and ~6% respectively. Zhao et al. [24] showed that in porous structures, the unit cell design affects the properties depending on the relative contribution of bending and buckling. For example, the cubic structure displays low ductility because the deformation is dominated by buckling; while under the same loading condition, the deformation in the topology optimised structure is determined by both bending and buckling. As the struts of cubic structure are parallel to loading direction, there is little bending stress; while the angle between the struts of topology optimised structure and loading direction is 45° [2], the topology optimised structure has higher bending stress than the cubic

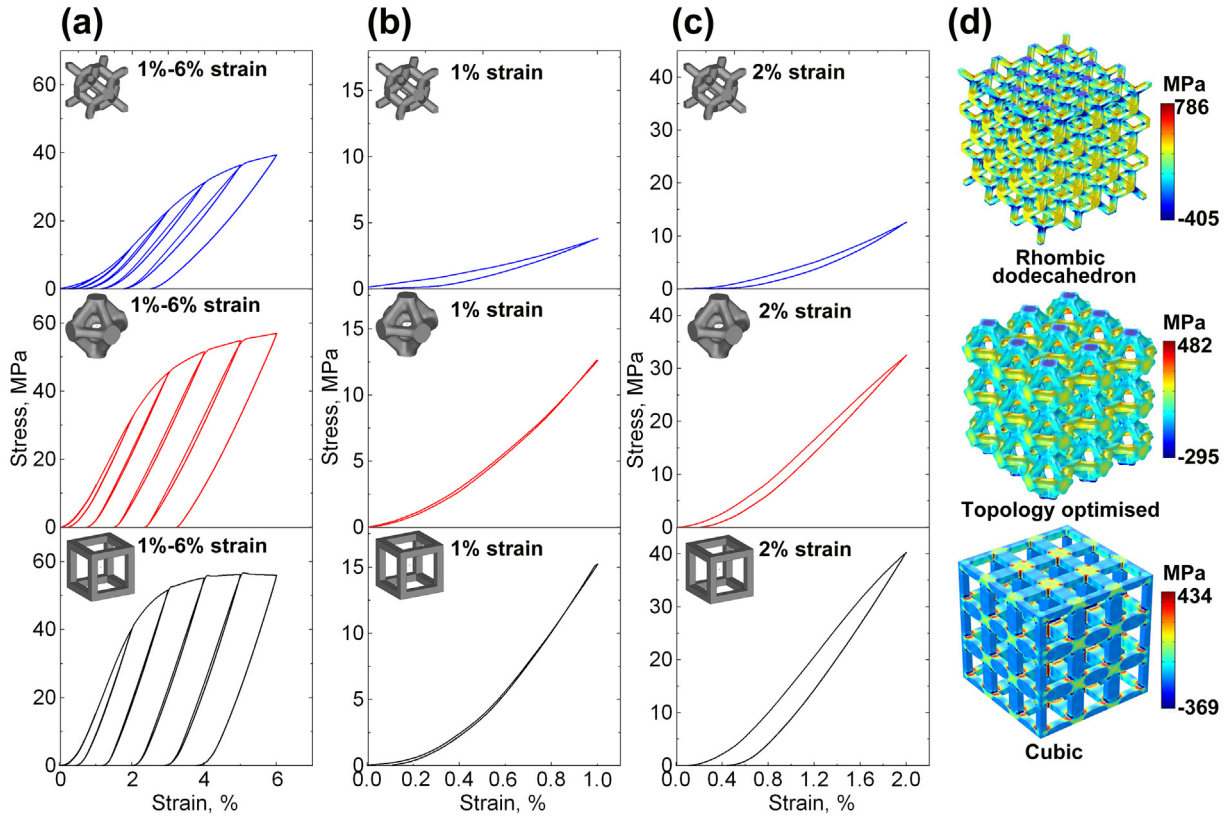

Fig. 2. The stress-strain curves for multiple cyclic load-unloading curves and FEM results for three structures: (a) the stress-strain curves at a range of 1–6% strain levels, (b) the stress-strain curves at 1% strain level, (c) the stress-strain curves at 2% strain level and (d) the FEM stress distribution at 1% strain level.